Macroscopic Klein tunneling in spin-orbit-coupled Bose-Einstein condensates

Dan-Wei Zhang, Zheng-Yuan Xue, Hui Yan, Z. D. Wang, and Shi-Liang Zhu

Phys. Rev. A **85**, 013628 — Published 19 January 2012

DOI: 10.1103/PhysRevA.85.013628

Macroscopic Klein Tunneling in spin-orbit coupled Bose-Einstein Condensates

Dan-Wei Zhang,[1,2] Zheng-Yuan Xue,[1] Hui Yan,[1] Z. D. Wang,[2,*] and Shi-Liang Zhu[1,†]

[1] *Laboratory of Quantum Information Technology and SPTE, South China Normal University, Guangzhou, China*

[2] *Department of Physics and Center of Theoretical and Computational Physics, The University of Hong Kong, Pokfulam Road, Hong Kong, China*

We propose an experimental scheme to detect the macroscopic Klein tunneling with spin-orbit coupled Bose-Einstein condensates (BECs). We show that a nonlinear Dirac equation with tunable parameters can be realized with such BECs. Through numerical calculations, we demonstrate that the macroscopic Klein tunneling can be clearly detected under realistic conditions. The macroscopic quantum coherence in such relativistic tunneling is clarified and the BEC with a negative energy is shown to be able to transmit transparently through a wide Gaussian potential barrier.

PACS numbers: 07.35.Mn, 03.75.Lm, 71.70.Ej, 03.65.Pm

I. INTRODUCTION

Shortly after the relativistic equation of electron was established by Dirac, Klein used it to study an electron scattering by a potential step and found that there exists a nonzero transmission probability even though the potential height tends to infinity[1], in contrast to the scattering of a non-relativistic particle. This phenomena has been referred to as the Klein tunneling (KT). The KT is an intrinsic relativistic effect and is interpreted as a fundamental property of Dirac equation that particle and antiparticle states are inherently linked together as two components of the same spinor wavefunction [2].

This unique scattering process has attracted lots of interest over the past eighty years but failed to be directly tested by elementary particles due to the requirements of currently unavailable electric field gradients [3]. Interestingly, the dynamics of particles in some systems, such as electrons in graphene [3] and trap ions [4, 5] etc., may be described by effective relativistic wave equations and have been proposed to observe such relativistic tunneling. Ultra-cold atoms in optical lattices [6] and light-induced gauge fields [7] are also able to behave as relativistic particles [8, 9]. Recent experiments in graphene heterojunctions [10, 11] have provided some indications for KT. However, the existence of disorders and interactions in these solid-state systems makes it hard to realize full ballistic scatterings. In addition, it seems hard to unambiguously observe the KT in the graphene since it is a typical 2D system, while the scattering in the 2D system is a combination of perfect transmission for normally incident particles (a relativistic effect) and exponentially decay tunneling for obliquely incident particles (a non-relativistic effect). **Moreover, Klein tunneling as well as Zitterbewegung effect have been experimentally simulated with the trapped ions[5]**.

In this paper we propose a feasible experimental scheme to observe macroscopic KT with spin-orbit coupled BECs [12, 13]. We demonstrate that a one-dimensional nonlinear Dirac equation (NLDE) with tunable parameters can be realized with a spinor BEC in the presence of a light-induced gauge field. Through numerical simulations, we demonstrate that a macroscopic KT can be observed under realistic conditions. The simple configuration of gauge field, in combination with controllable dimensions, interactions and potential barriers may provide us with a clean and tunable platform to investigate the interesting relativistic tunneling effects.

We investigate the relativistic tunneling of a macroscopic quantum object by comparing the transmission coefficients between a BEC in the absence of interactions and an incoherent ensemble average of non-condensed atoms. In addition, we find that a realistically weak interaction between atoms affects slightly the transmission coefficients. The main feature of a BEC is that all atoms in the BEC are in the same state and with the same phase and then the BEC can be considered as a macroscopic object. So the tunneling of a BEC we studied is a coherent scattering of a macroscopic object. The tunneling in the former shows a distinct difference of the relativistic effects between the macroscopic objects and the ensemble average of some microscopic particles, while the KT is only studied previously within a single-particle scenario. We also present another unexpected result that the BEC with a negative energy can almost completely transmit through a Gaussian barrier. Since KT is a relativistic phenomenon associated with an anti-particle in the potential, our proposed spin-orbit coupled BEC can mimic a macroscopic 'anti-BEC' (a super-atom made from 'anti-atoms'), at least in a scattering problem. Therefore, the mimicked 'anti-BEC' may open the possibility to explore exotic relativistic effects of macroscopic body (even for very large antimatter), in contrast to a conventional wisdom that relativistic effects are only clearer for a microscopic particle.

The paper is organized as follows. In Sec. II we propose an approach to realize a spin-orbit cou-

*Electronic address: zwang@hku.hk

†Electronic address: slzhu@scnu.edu.cn

pled atomic gas through the Λ-level configuration, and then demonstrate that the dynamics of the atoms should be described by the NLDE when the atoms are condensed into a BEC. In Sec. III we show that the region for KT of a single atom can be reached in experiments. Then we demonstrate in Sec. IV that the KT of BECs can be clearly observed. We also clarify the macroscopic quantum coherence in such relativistic tunneling and show that a wide Gaussian potential barrier is transparent for the BEC with a negative energy. In Sec. V, we present our discussion and conclusion. In the appendix, we briefly review the numerical method to calculate the transmission coefficient of a single atom scattered by a Gaussian potential.

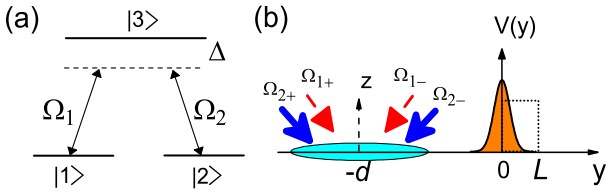

FIG. 1: (color online). Schematic illustration of the system. (a) Atom with Λ-level configuration interacting with laser beams characterized by the Rabi frequencies Ω_1, Ω_2 and a large detunning Δ. (b) The configuration of the laser beams to realize a Dirac-like equation by the lasers Ω_1,Ω_2 and an effective Gaussian (square)-shape potential induced by another laser beam. The atoms are confined in a 1D waveguide along y axis and scattered by the potential.

II. REALIZATION OF A NONLINEAR DIRAC EQUATION WITH COLD ATOMS

The Dirac equation with tunable parameters can be realized with ultrcold atoms through two different approaches [6, 8, 9]. Similar to graphene, it was proposed that the low energy quasi-particles in a honeycomb optical lattice should also be described by the relativistic Dirac equation [6]. On the other hand, the Hamiltonian of cold atoms (without optical lattices) with certain spin-orbit coupling, which can be achieved with synthetic gauge fields, is a Dirac Hamiltonian when the wave number of the atoms is much smaller than the wave number of the laser beams. It is demonstrated that the required spin-orbit coupling can be realized though a tripod level configuration [8, 9]. In this paper we proposed that the Λ-level configuration is also feasible to be used in the realization of Dirac equation.

Let us consider the motion of bosonic atoms with mass m in y-z plane with each having a Λ-level structure interacting with laser beams as shown in Fig.1. The ground states $|1\rangle$ and $|2\rangle$ are coupled to an excited state $|3\rangle$ through laser beams characterized respectively with the Rabi frequencies $\Omega_1 = \Omega\cos(\kappa_y y)e^{-i\kappa_z z}$ and $\Omega_2 = \Omega\sin(\kappa_y y)e^{i(\pi-\kappa_z z)}$, where $\Omega = \sqrt{|\Omega_1|^2+|\Omega_2|^2}$. As shown in Fig.1 (b), the Rabi frequencies Ω_1 and Ω_2 can be respectively realized with a pair of lasers $\Omega_{1\pm} = \frac{1}{2}\Omega\exp[i(-\kappa_z z \pm \kappa_y y)]$ and $\Omega_{2\pm} = \frac{1}{2}\Omega\exp\{i[-\kappa_z z \pm (\kappa_y y+\pi/2)]\}$, where $\kappa_y = \kappa\cos\varphi$ and $\kappa_z = \kappa\sin\varphi$ with κ being the wave number of the lasers and φ being the angle between the laser and the y axis. The Hamiltonian of a single atom reads $H = \frac{\mathbf{P}^2}{2m} + V(\mathbf{r}) + H_I$, where $V(\mathbf{r}) = \sum_{j=1}^{3}(V_T(\mathbf{r}) + V_b(\mathbf{r}))|j\rangle\langle j|$ denotes the full external potentials (including the trapping potentials V_T and the scattering potential V_b) and the interaction Hamiltonian $H_I = \hbar\Delta|3\rangle\langle 3| - (\sum_{j=1}^{2}\hbar\Omega_j|3\rangle\langle j| + h.c.)$ with Δ as the detuning. Diagonalizing H_I yields the eigenvalues as $\hbar\{[\Delta - \sqrt{\Delta^2+4\Omega^2}]/2, 0, [\Delta+\sqrt{\Delta^2+4\Omega^2}]/2\}$. In the large detuning case, the two eigenstates corresponding to the first two eigenvalues span a near-degenerate subspace, and can be considered as a pseudo-spin with spin-orbit coupling induced by a gauge potential [7, 14]. Under this condition we obtain an effective Hamiltonian

$$H = \frac{p_y^2+p_z^2}{2m} + v_y\sigma_y p_y + v_z\sigma_z p_z + \gamma_z\sigma_z + V_T + V_b, \quad (1)$$

where $v_y = \frac{\hbar\kappa_y}{m}$, $v_z = \frac{\hbar\kappa_z\Omega^2}{2m\Delta^2}$, and $\gamma_z = \frac{\hbar^2\Omega^2}{4m\Delta^2}[\kappa_y^2 - (1+\Omega^2/\Delta^2)\kappa_z^2] + \frac{\hbar\Omega^2}{2\Delta}$. In the derivation, we have dropped an irrelevant constant and assumed that the potentials $V(\mathbf{r})$ are spin-independent. Furthermore, the atomic gas can well be confined by a 1D optical waveguide along y axis [9], so we may further restrict our study in 1D system. Therefore, both tripod and *Lambda*-level configuration can be used, in principle, in the realization of the Dirac equation. Comparing with the tripod configuration [8, 9], the large detuning is necessary in the *Lambda* configuration. However, the laser beams are simpler in the lambda level configuration. Furthermore, the pseudospins in the lambda configuration would be more robust against the collision of the atoms since they are constructed by the lowest two dressed states, while the two dark states in the tripod configuration are not the ground states.

We assume that the interaction can be described by an effective 1D interacting strength $g = 2\hbar^2 a_s N/(m l_\perp^2)$, where a_s is the scattering length, N is the particle number, and $l_\perp$ is the oscillator length associated to a harmonic vertical confinement. The interaction between the atoms (per particle) should be much smaller than the confinement frequency (about kHz)[20], and thus is also much smaller than Ω (about MHz), therefore the interaction can not pump the atoms outside of the near-degenerate subspace. Under the condition $p_y \ll \hbar\kappa_y$, we can safely neglect the p_y^2 term. In addition, we assume that the bosonic atoms are condensed into a BEC state. Within the Gross-Pitaevskii formalism, the interacting bosons in the near-degenerate subspace are then effectively described by a 1D NLDE as $i\hbar\partial_t\Psi = H_{ND}\Psi$ [15], where

$$H_{ND} = -i\hbar v_y\sigma_y\partial_y + \gamma_z\sigma_z + g\Psi^\dagger\cdot\Psi + V_T + V_b \quad (2)$$

with v_y being the effective speed of light and γ_z as the

effective rest energy of the cold atoms. It is a remarkable feature that all parameters, v_y, γ_z and g, can be experimentally controllable, providing us with a tunable platform to explore the relativistic quantum effects.

III. KLEIN TUNNELING OF A SINGLE ATOM

We now turn to address the relativistic quantum tunneling that can be observed with cold atoms. To have an intuitive physics picture, we first consider a single atom with energy E scattered by a square potential with the width L and potential height V_s. Such potential can be experimentally formed by a laser beam with flat-top profile [16]. The transmission coefficient T_D for the so-called KT regime $V_s > E + \gamma_z$ [2], can be obtained explicitly as

$$T_D = \left[1 + (\eta - \eta^{-1})^2 \sin^2(\beta L)/4\right]^{-1}, \qquad (3)$$

where $\eta = \sqrt{\frac{(V_s - E + \gamma_z)(E + \gamma_z)}{(E - V_s + \gamma_z)(\gamma_z - E)}}$ and $\beta = \sqrt{\frac{(V_s - E - \gamma_z)}{(V_s - E + \gamma_z)}}/\hbar$. Comparing with the well-known property in the non-relativistic quantum mechanics that the transmission coefficient decreases mono-exponentially with the height V_s or width L, a distinctly different feature within this KT region is that the tunneling amplitude is an oscillation function of V_s or L even when the kinetic energy of the incident particle is less than the height of the barrier. This relativistic effect can be attributed to the fact that the incident particle in a positive energy state can propagate inside the barrier by occupying a negative energy state, which is also a plane wave aligned in energy with that of the particle continuum outside. Matching between positive and negative energy states across the barrier leads to the high-probability tunneling. We take the atoms of ^{7}Li as an example. If we choose the following practical parameters: $\kappa_y = 10^7$ m^{-1}, $\kappa_z = 0.8 \times 10^7$ m^{-1}, $\Omega = 10^7$ Hz and $\Delta = 10^9$ Hz, it is found that the Klein regime corresponds to the Rabi frequency $\Omega_b^s > 0.162$ MHz, which can be easily achieved in experiments. So we have demonstrated from a simple example that it is feasible to observe the KT with cold atoms.

IV. KLEIN TUNNELING OF ATOMIC CONDENSATES

As for a practical experiment it is required to release two conditions: the trajectory of a single atom is hard to detect, and it is much easier to measure the density evolution of an ensemble of atoms in experiments. Compared with the square potential, a Gaussian potential $V_b^{\rm G}(y,\nu) = \nu V_{\rm G} e^{-y^2/\sigma^2}$, where $V_{\rm G}$ is the height and σ characterizes the spatial variance, is much easier to be generated. Here ν donates a barrier ($\nu = +$) or a potential well ($\nu = -$), and the potential barrier (well) can be realized by focusing a blue- (red-) detuned far-off-resonant Gaussian shaped laser beam. However, the conditions of resonant transmission vary with the velocity and the width of the potential, and thus both the ensemble of atoms and the Gaussian potential may smoothen the oscillations in the transmission coefficient. So it is natural to ask whether the KT can still be observed in an ensemble of atoms. Surprisingly we will illustrate below that the KT of the BEC may be observed very clearly.

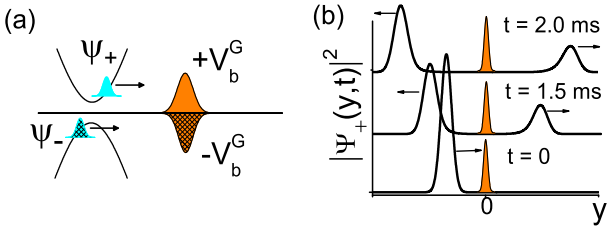

FIG. 2: (color online). (a) A schematic diagram shows four kinds of scattering events. (b) Normalized density distribution in a scattering process at time $t = 0$, 1.5 and 2.0 ms. The peaks at $y = 0$ are the Gaussian barriers.

We assume that the BEC consisted of ^{7}Li is initially trapped in a harmonic trap which moves along the y axis. At the initial time $t = 0$, the center of the trap locates at $y = -d$, and the center of the Gaussian potential is at $y = 0$. The trap is turned off at $t = 0$ and then we calculate the evolution of the density profile of the atomic gas after a long enough time for scattering. The single-atom dispersion described in Eq. (2) is characterized by two branches $E_\pm(k_y) = \pm(\gamma_z^2 + \hbar^2 v_y^2 k_y^2)^{1/2}$, where the lower (up) branch represents the negative (positive) energy state. One can prepare an initial BEC with a designated mode k_0 at the positive or negative energy branch. The two branches allow us to study a more fruitful tunneling problem: there are four classes of the scattering which describe the wave function Ψ_μ ($\mu(=\pm)$) scattered by the potential $V_b^G(y,\nu)$,as shown in Fig. 2(a).

The BEC in a harmonic trap can be well described by a Gaussian wave packet, so we may choose the initial wave function as

$$\Psi_\mu(y,0) = \frac{1}{\sqrt{l_0\sqrt{\pi}}} e^{i\mu k_0 y} e^{-(y+d)^2/2l_0^2} \phi_\mu, \qquad (4)$$

where l_0 is the width, k_0 is the central wave number of the wave-packet and the spinor ϕ_μ are defined as $\phi_+ = (i\cos\xi, -\sin\xi)^T$, $\phi_- = (-i\sin\xi, \cos\xi)^{Tr}$ with $\xi = \frac{1}{2}\arctan(\hbar v_y k_0/\gamma_z)$ and Tr as the transposition of matrix. This wave function describes a Gaussian wave packet with the central velocity $\hbar(\kappa_y + \mu k_0)/m$ moving along y-axis. After the evolution governed by Dirac-type Eq. (2) with time t, the finial wave function becomes

$$\Psi_\mu(y,t) = \hat{\mathcal{T}} \exp\left(-\frac{i}{\hbar}\int_0^t H_{ND} dt\right) \Psi_\mu(y,0), \qquad (5)$$

where $\hat{\mathcal{T}}$ denotes the time ordering operator. **We numerically calculate $\Psi_\mu(y,t)$ in Eq.(5) by using the standard split-operator method. According to**

the method [19], Eq. (5) can be rewritten as

$$\Psi_\mu(y,t+\delta t)=\Big\{e^{-\frac{i}{2\hbar}v_y\sigma_y p_y\delta t}e^{-\frac{i}{\hbar}\gamma_z\sigma_z\delta t}\times e^{-\frac{i}{\hbar}\left[V_b^{\rm G}(y,\nu)+g|\Psi_\mu(y,t)|^2\right]\delta t}\times e^{-\frac{i}{2\hbar}v_y\sigma_y p_y\delta t}+\mathcal{O}(\delta t^3)\Big\}\Psi_\mu(y,t). \tag{6}$$

In the sufficiently short time step δt, the high-order term $\mathcal{O}(\delta t^3)$ (due to the non-commuting) can be safely neglected. Combining with the Fourier transform between the position and momentum spaces, we can finally get the numerical solution of $\Psi_\mu(y,t)$ following the computation procedure step by step with time step δt.

We have numerically calculated $\Psi_\mu(y,t)$, and found the existence of stationary solution for the scattering process, with an example being shown in Fig. 2(b). After tunneling, the incident wave packet divides into the left- and right-traveling wave packets and only the latter one is on the transmission side of the barrier. Thus we can define the transmission coefficient of the incident wave packet $\Psi_\mu(y,0)$ scattering by a potential $V_b^G(y,\nu)$ as

$$T_{\mu\nu}=\int_\sigma^\infty \Psi_\mu^\dagger(y,\tau)\Psi_\mu(y,\tau)dy, \tag{7}$$

where τ (being slightly larger than d/v_0) represents a time that the reflected and transmitted wave packets are sufficient away from the Gaussian potential. One can directly measure the transmission coefficient in Eq. (7) since the spatial density distribution $\rho_\mu(y,\tau)=|\Psi_\mu(y,\tau)|^2$ can be detected using absorption imaging [17].

We first look into the tunneling phenomena for a BEC in the absence of interactions ($g=0$). We note that there are two identities $T_{++}=T_{--}$ and $T_{-+}=T_{+-}$ since Eq.(2) with $g=0$ is invariant under the charge conjugation [18]. We plot the transmission coefficient T_{++} as a function of the height $V_{\rm G}$ and width σ in Fig. 3(a) with the practical parameters. It is interesting to note that the transmission coefficient decreases exponentially to zero with $V_{\rm G}$ when $V_{\rm G}<V_{\rm G}^K$, while it will increase and then be an oscillating function in the Klein region $V_{\rm G}>V_{\rm G}^K$, being similar to the results of Eq. (3) for the square barrier. Here the critical value of the potential height may approximately be estimated using the square barrier with $V_{\rm G}^K=E(k_0)+\gamma_z\approx 0.09$ MHz. Moreover, the feature $T_{++}=T_{--}$ is also confirmed in the insert of Fig. 3(a). As for the transmission coefficient $T_{++}(\sigma)$, we may obtain several tunneling oscillations with the potential width, but it decreases to zero when the width is further increased. Although the amplitude of tunneling oscillation is less than the unit as comparing with the tunneling of single atom, the amplitude of tunneling oscillation can be more than 0.5 and meanwhile the period can be a few micrometers, which is experimentally detectable.

Another interesting feature induced by the relativistic effects is that, the BEC with negative energy can almost completely transmit a wide Gaussian potential barrier, as shown in Fig. 3(b). The transmission coefficient T_{-+} is an oscillating function of the potential width σ when σ is smaller than 3 μm, while it saturates quickly to the unit when the potential width is larger than 3 μm, leading to an unexpected result that a wide Gaussian potential barrier is actually totally transparent for a BEC. This phenomenon can be understood through the fact that such scattering feature is actually equivalent to that of a BEC of positive energy scattered by a Gaussian potential well because of $T_{-+}=T_{+-}$. We also calculate the transmission coefficient for the central mode of the wave packet, as shown in the insert of Fig. 3(b), which further confirms that a wide enough Gaussian potential well is transparent. The reason lies in the fact that, in contrast to the periodic function (without a saturation value) in a square potential well, the Gaussian potential well is smooth in the whole space, and then even support adiabatic motions of wave packets in the large width limit.

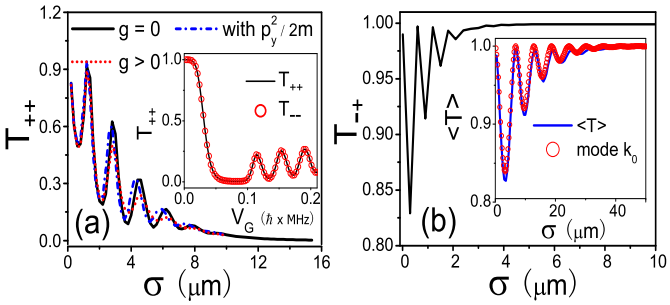

FIG. 3: (color online). KT of BECs. (a) $T_{++}(\sigma)$ for $V_{\rm G}/\hbar=0.2$ MHz and $T_{++}(V_G)$ (insert) for $\sigma=5$ μm. The tunnelings of a BEC with the classic kinetic energy term and the conventional atomic interaction ($N=2\times10^4$, $l_\perp=1.4$ μm and $a_s=5a_0$ with a_0 being the Bohr radius) are also depicted. (b) The coefficients $T_{-+}(\sigma)$, $\langle T(\sigma)\rangle$ (insert) of one atom with central mode k_0, and of 10^4 atoms for $V_{\rm G}/\hbar=0.2$ MHz. The other parameters in (a) and (b) are $l_0=10$ μm, $k_0=5.5\times10^5$ m^{-1}, $\gamma_z/\hbar=30$ kHz, and $d=4(l_0+\sigma)$.

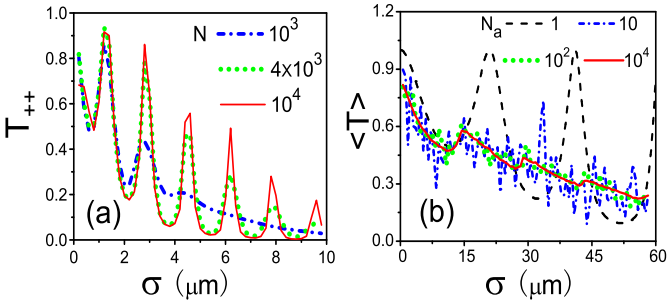

FIG. 4: (color online). Comparing KT of BECs with that of an ensemble of non-condensed atoms. (a) $T_{++}(\sigma)$ with $N=10^3$, 4×10^3, 10^4 are shown by fixing the energy E_{int} for $l_0=10$ μm and $d=4(l_0+\sigma)$. (b) $\langle T(\sigma)\rangle$ with $N_a=1$, 10, 10^2, and 10^4 atoms for $\sigma_k=5\times10^5$ m^{-1}. The other parameters in (a) and (b) are $V_{\rm G}/\hbar=0.2$ MHz, $k_0=5.5\times10^5$ m^{-1}, and $\gamma_z/\hbar=30$ kHz.

The tunneling properties exhibited in Fig. 3(a,b) are intrinsic relativistic and macroscopic quantum phenomena that can not be explained with an incoherent ensemble average of many atoms. To clarify this point, we calculate the average transmission coefficients for an ensemble of N_a noninteracting atoms defined as

$$\langle T\rangle = \frac{1}{N_a}\sum_{i=1}^{N_a} T(k_i), \tag{8}$$

where $T(k_i)$ donates the transmission coefficient for the atom i with the wave number k_i scattered by the potential. The numerical calculation method for $T(k_i)$ is given in the Appendix. Here we choose k_i to be the same Gaussian distribution as that of the initial BEC wave function $\Psi_\mu(y,0)$, i.e., $k_i \sim N(k_0,\sigma_k^2)$ with the variance $\sigma_k = 1/l_0$. The $\langle T\rangle$ of 10^4 atoms is shown in the insert of Fig. 3(b), which is almost the same as that of a single atom since σ_k is small. The differences between $\langle T\rangle$ and T_{-+} in Fig. 3(b) demonstrate that the tunneling of BEC is not equivalent to an ensemble average of the individual atoms even with the same distribution of wave number. The coefficient $\langle T\rangle$ represents an incoherent transmission of the individual particles since it is a sum of the transmission coefficients of all particles. In contrast, the phases of all atoms in the BEC are the same and then the transmission of a BEC is coherent. The coherent transmission in BEC and incoherence in $\langle T\rangle$ cause the difference in Fig. 3. The same phase for all particles in BEC is stemmed from that macroscopic number of particles are condensed in the same state, so the coherent transmission of BEC may be called as a macroscopic quantum tunneling.

To clarify further the macroscopic quantum phenomena in the relativistic tunneling of a BEC, we compare the scaling properties of transmission coefficients for a weakly interacting BEC and an incoherent ensemble average of atoms. An example of scaling of T_{++} is plotted in Fig. 4(a). In the calculations, we have fixed the weak interatomic interaction energy $E_{int} \approx g/l_0$ and kept the parameter $\gamma = mgl_0/N\hbar^2 \ll 1$ [20] for $l_0 = 5$ μm when $N = 10^3$, $l_\perp = 1.4$ μm and $a_s = 5a_0$ ($\gamma \sim 10^{-3}$), both of which restrict our discussions in the regime for 1D BECs where the Dirac dynamics instead of the nonlinear dynamics dominates. In this case, the increase of particle number is achieved by proportionally increasing the length l_0 of the BEC with small γ. For comparison, we also calculate the scaling of $\langle T\rangle$ for the atom number of one (with $k_i = k_0$), 10, 10^2, 10^4 in Fig. 4(b). Comparing Fig. 4(a) with Fig. 4(b), a distinct difference of the BEC and an ensemble average of the individual atoms is that, the coefficient T_{++} enhances with the increasing of the atomic number of the BEC, while the coefficient $\langle T\rangle$ decreases with the increasing of the atomic number. However, in order to keep the same interaction parameter in the above calculation, we have increased simultaneously the particle number and the width of the Gaussian wave packet. In this way the momentum distribution of the wave functions is shrunk, which is a dominant reason for the above scaling feature. So many atoms may condense into the same momentum state is essential in the observation of KT of the BEC.

V. DISCUSSION AND CONCLUSION

Before concluding, we wish to make two additional comments. (i) To judge the feasibility of the Dirac approximation in Eq.(2), the coefficients T_{++} with or without the quadratic term are compared in Fig. 3(a). It is shown that the quadratic term leads to merely a slight left-shift of the tunneling peaks. This phenomenon can be interpreted by the fact that the wavelength of the BEC inside the barrier decreases slightly in the presence of the additional low kinetic energy. This result verifies that the approximation led to the Dirac equation is well satisfied. **(ii) In Fig. 3(a), we have also calculated the transmission coefficient for BECs with conventional atomic interactions without Feshbach resonance, in which case the experimental setup can be simplified. The result shows that the effect of the realistically weak interaction is little and smooths merely the tunneling oscillation slightly. Therefore the exotic tunneling phenomena addressed here survive in the case of weak interaction between atoms.**

In summary, we have proposed an experimental scheme to detect macroscopic KT using the spin-orbit coupled BEC. Through numerical simulations, we have elaborated that such macroscopic KT can be observed under realistic conditions. In view of that the spin-orbit coupled BEC has been realized in a very recent experiment [13], it is anticipated that the present proposal will be tested by a near future experiment.

VI. ACKNOWLEDGMENTS

This work was supported by the NSFC (Nos. 11125417 and 10974059), the SKPBR (No.2011CB922104), the GRF and CRF of the RGC of Hong Kong.

Appendix: The derivation of $T(k_i)$ in Eq.(8)

The Dirac equation for a particle scattering by a Gaussian potential can not be solved analytically for the incoming atom with energy $E_i = \sqrt{(\hbar v_y k_i)^2 + \gamma_z^2}$ and momentum $p_i = \hbar k_i$. However, we here adopt an efficient method to numerically solve it based on the transfer matrix methods [9]. The numerical procedures are outlined as follows. One first cuts the Gaussian potential into spatially finite range $y \in [-y_c, y_c]$, where the cutoff position y_c should be chosen to guarantee that the potential height outside the range is low enough to be transparent for the atoms,

i.e., $V_b^{\rm G}(y_c) \ll E_i, V_{\rm G}$. Secondly, one equally divides this range into n spindly segments and each segment can be considered as a square potential if n is large enough. The potential height of j-th ($j = 1, 2, \cdots, n$) square potential is given by $V_j = V_b^{\rm G}(y_j + f/2)$ with $y_j = -y_c + (j-1)f$ and the width of each potential $f = 2y_c/n$. In this case, the Gaussian potential can be approximately viewed as a sequence of connective small square potential barriers, and thus the transmission coefficient $T(k_i) \approx 1/|m_{11}|^2$, where m_{11} is the first element of the whole transfer matrix $M = M_n M_{n-1} \cdots M_j \cdots M_2 M_1$. Here M_j denotes the transfer matrix of the j-th square potential barrier, whose explicit elements are given by [9]

$$\begin{aligned}
(M_j)_{11} &= (\cos\tfrac{p_j f}{\hbar} + i\tfrac{\kappa^2+\kappa_j^2}{2\kappa\kappa_j}\sin\tfrac{p_j f}{\hbar})e^{-\frac{i}{\hbar}p_i f},\\
(M_j)_{12} &= (i\tfrac{\kappa_j^2-\kappa^2}{2\kappa\kappa_j}\sin\tfrac{p_j f}{\hbar})e^{-\frac{i}{\hbar}p_i(y_j+y_{j+1})},\\
(M_j)_{21} &= (M_j)_{12}^*,\\
(M_j)_{22} &= (M_j)_{11}^*,
\end{aligned} \tag{9}$$

where $\kappa = (E_i - \gamma_z)/(v_y p_i)$ and $\kappa_j = (E_i - \gamma_z - V_j)/(v_y p_j)$ with $(E_i - V_j)^2 = v_y^2 p_j^2 + \gamma_z^2$. Note that this numerical calculation scheme recovers the non-relativistic scattering governed by the Schrödinger equation.

[1] O. Klein, Z. Phys. **50**, 157 (1929).

[2] N. Dombey and A. Calogeracos, Phys. Rep. **315**, 41 (1999).

[3] M.I. Katsnelson, K.S. Novoselov, and A.K. Geim, Nature Phys. **2**, 620 (2006); V.Jakubsky, L. M. Nieto, and S. Plyushchay, Phys. Rev. D **83**, 047702 (2011).

[4] L. Lamata, J. León, T. Schätz, and E. Solano, Phys. Rev. Lett. **98**, 253005 (2007).

[5] R. Gerritsma, G. Kirchmair, F. Zahringer, E. Solano, R. Blatt, C. F. Roos, Nature (Landon) **463**, 68 (2010); R. Gerritsma, B. P. Lanyon, G. Kirchmair, F. Zahringer, C. Hempel, J. Casanova, J. J. Garcia-Ripoll, E. Solano, C. F. Roos Phys. Rev. Lett. **106**, 060503 (2011).

[6] S.L. Zhu, B. Wang, and L.M. Duan, Phys. Rev. Lett. **98**, 260402 (2007); I.I. Satija, D. C. Dakin,J. Y. Vaishnav, and C.W. Clark, Phys. Rev. A **77**, 043410 (2008) C. Chamon,C.-Y. Hou, R. Jackiw, C. Mudry, S.-Y. Pi, and G. Semenoff, Phys. Rev. B **77**, 235431 (2008).

[7] J. Ruseckas, G. Juzeliunas, and M. Fleischhauer, Phys. Rev. Lett. **95**, 010404 (2005); S.L. Zhu, H. Fu, C. J. Wu, S. C. Zhang, and L. M. Duan, *ibid.*, **97**, 240401 (2006).

[8] J.Y. Vaishnav and C.W. Clark, Phys. Rev. Lett. 100, 153002 (2008); G. Juzeliūnas, J. Ruseckas, M. Lindberg, L. Santos, and P. Öhberg, Phys. Rev. A **77**, 011802(R) (2008).

[9] S.L. Zhu, D.W. Zhang, and Z.D. Wang, Phys. Rev. Lett. **102**, 210403 (2009).

[10] N. Stander, B. Huard, and D. Goldhaber-Gordon, Phys. Rev. Lett. **102**, 026807 (2009).

[11] A.F. Young and P. Kim, Nature Phys. **5**, 222 (2009).

[12] T.D. Stanescu, B. Anderson, and V. Galitski, Phys. Rev. A **78**, 023616 (2008); C.-J. Wang, C. Gao, C.-M. Jian and H. Zhai, Phys. Rev. Lett. **105**, 160403 (2010); T.L. Ho and S. Zhang, arXiv:1007.0650.

[13] Y.J. Lin, K. Jimenez-Carcia, and I.B. Spielman, Nature (London) **471**, 83 (2011).

[14] X.-J. Liu, M. F. Borunda, X. Liu and J. Sinova, Phys. Rev. Lett. **102**, 046402 (2009); C. Zhang, Phys. Rev. A **82**, 021607(R) (2010).

[15] M. Merkl, A. Jacob, F.E. Zimmer, P. Öhberg and L. Santos, Phys. Rev. Lett. **104**, 073603 (2010).

[16] M.G. Tarallo, J. Miller, J.Agresti, E. D'Ambrosio, R. DeSalvo, D. Forest, B. Lagrange, J. M. Mackowsky, C.Michel, J.L. Montorio , N. Morgado, L. Pinard, A. Remilleux, B. Simoni, P. Willems Appl. Opt, **46**, 26 (2007).

[17] L. Khaykovich, F. Schreck, G. Ferrari, T. Bourdel, J. Cubizolles, L.D. Carr, Y. Castin and C. Salomon Science **296**, 1290 (2002).

[18] N. Dombey, P. Kennedy, and A. Calogeracos, Phys. Rev. Lett. **85**, 1787 (2000).

[19] J. Larson and E. Sjoqvist, Phys. Rev. A 79, 043627 (2009), and the references there in.

[20] D.S. Petrov, G.V. Shlyapnikov, and J.T.M. Walraven, Phys. Rev. Lett. **85**, 3745 (2000).